

1 **O-GlcNAcylation of SAMHD1 Indicating a Link between Metabolic Reprogramming**  
2 **and Anti-HBV Immunity**

3  
4 **Running Title: O-GlcNAcylation of SAMHD1 inhibits HBV**

5  
6 Jie Hu<sup>1,#</sup>, Qingzhu Gao<sup>1,#</sup>, Yang Yang<sup>1,#</sup>, Jie Xia<sup>1,#</sup>, Wanjun Zhang<sup>2</sup>, Yao Chen<sup>1</sup>, Zhi Zhou<sup>1</sup>,  
7 Lei Chang<sup>2</sup>, Yuan Hu<sup>1</sup>, Hui Zhou<sup>3</sup>, Li Liang<sup>1</sup>, Xiaosong Li<sup>4</sup>, Quanxin Long<sup>1</sup>, Kai Wang<sup>1, \*</sup>,  
8 Ailong Huang<sup>1, \*</sup>, Ni Tang<sup>1, \*</sup>

9 <sup>1</sup>Key Laboratory of Molecular Biology for Infectious Diseases (Ministry of Education),  
10 Institute for Viral Hepatitis, Department of Infectious Diseases, The Second Affiliated  
11 Hospital, Chongqing Medical University, Chongqing, China.

12 <sup>2</sup>State Key Laboratory of Proteomics, Beijing Proteome Research Center, National Center  
13 for Protein Sciences (Beijing), Beijing Institute of Lifeomics, Beijing, China.

14 <sup>3</sup>School of Pharmaceutical Science, Chongqing Medical University, Chongqing, China.

15 <sup>4</sup>The First Affiliated Hospital, Chongqing Medical University, Chongqing, China.

16

17 **\*Correspondence**

18 Ni Tang, Ailong Huang, Kai Wang, Key Laboratory of Molecular Biology for Infectious  
19 Diseases (Ministry of Education), Institute for Viral Hepatitis, Department of Infectious  
20 Diseases, The Second Affiliated Hospital, Chongqing Medical University, Chongqing, China.

21 Phone: 86-23-68486780, Fax: 86-23-68486780,

22 E-mail: nitang@cqmu.edu.cn (N.T.), ahuang@cqmu.edu.cn (A.L.H.),

23 wangkai@cqmu.edu.cn (K.W.)

24 #These authors contributed equally to this work.

25 **Character count: 7465**

26 **Abstract**

27 Viruses hijack the host cell machinery to promote viral replication; however, the mechanism  
28 by which metabolic reprogramming regulates innate antiviral immunity in the host remains  
29 elusive. Herein, we found that Hepatitis B virus (HBV) infection upregulates glucose  
30 transporter 1 expression, promotes hexosamine biosynthesis pathway (HBP) activity, and  
31 enhances O-linked  $\beta$ -N-acetylglucosamine (O-GlcNAc) modification of downstream proteins.  
32 HBP-mediated O-GlcNAcylation positively regulates host antiviral response against HBV *in*  
33 *vitro* and *in vivo*. Mechanistically, O-GlcNAc transferase (OGT)-mediated O-GlcNAcylation  
34 of sterile alpha motif and histidine/aspartic acid domain-containing protein 1 (SAMHD1) on  
35 Ser93 stabilizes SAMHD1 and enhances its antiviral activity. In addition, O-GlcNAcylation of  
36 SAMHD1 promoted its antiviral activity against human immunodeficiency virus-1 *in vitro*. In  
37 conclusion, the results of our study reveal a link between HBP, O-GlcNAc modification, and  
38 innate antiviral immunity by targeting SAMHD1. Therefore, the results of this study  
39 demonstrate a strategy for the potential treatment of HBV infection by modulating HBP  
40 activity.

41

42 **Keywords:** Hepatitis B virus / O-linked  $\beta$ -N-acetylglucosamine modification / sterile alpha  
43 motif and histidine/aspartic acid domain-containing protein 1 / antiviral immunity  
44 /Hexosamine biosynthetic pathway

## 45 **Introduction**

46 Immunometabolism is an emerging field that highlights the importance of specific metabolic  
47 pathways in immune regulation. Metabolic enzymes, such as glyceraldehyde 3-phosphate  
48 dehydrogenase and pyruvate kinase isozyme M2 can directly modulate immune cell  
49 activation (Chang *et al*, 2013; Palsson-McDermott *et al*, 2015). In addition to providing  
50 energy and building blocks for biosynthesis, metabolites have been shown to participate in  
51 epigenetic modification and signaling transduction. the glycolytic product lactate not only  
52 regulates gene expression by histone acetylation (Zhang *et al*, 2019a), but also acts as a  
53 suppressor of type I interferon signaling by interacting with the mitochondrial antiviral  
54 signaling protein MAVS (Zhang *et al*, 2019b). Itaconate—another important metabolite for  
55 immune function—downregulates type I interferon signaling during viral infection by  
56 promoting alkylation of Kelch-like ECH-associated protein 1 and activation of  
57 anti-inflammatory proteins, including nuclear factor erythroid 2-related factor 2 (Mills *et al*,  
58 2018, 1; O'Neill & Artyomov, 2019).

59  
60 Viruses are obligate parasites that rely on the biosynthetic machinery of the host to complete  
61 their life cycle. They hijack the host cell machinery upon entry to fulfill their energetic and  
62 biosynthetic demands for viral replication. Human cytomegalovirus (HCMV) and herpes  
63 simplex virus-1 (HSV-1) remodel host cells to perform distinct, virus-specific metabolic  
64 programs (Vastag *et al*, 2011). HCMV reprograms host metabolism by upregulating the  
65 expression of carbohydrate-response element binding protein and glucose transporter 4  
66 (GLUT4) to provide materials for viral replication (Yu *et al*, 2014). Glucose uptake, glycolysis,  
67 and lipogenesis are enhanced in HCMV-infected cells to synthesize biomolecules. Moreover,  
68 HSV-1 promotes central carbon metabolism to synthesize pyrimidine nucleotides.

69

70 On the other hand, hosts may recognize virus-induced signaling and reprogram metabolic  
71 pathways to protect themselves from further damage. Increased glucose utilization,  
72 increased aerobic glycolysis, and inhibition of oxidative metabolism have emerged as the  
73 hallmarks of macrophage activation (Jung *et al*, 2019). Pattern recognition molecules as well  
74 as several metabolic pathways and metabolites have been reported to play an important role  
75 in regulating host innate immune response (Haskó & Cronstein, 2004; Skelly *et al*, 2019;  
76 Tsalikis *et al*, 2013). Therefore, it is important to identify the key metabolites that regulate  
77 innate immune response during viral infection. Understanding the relationship between cell  
78 metabolism, innate immunity, and viral infection may provide insights to develop new  
79 therapeutic targets to control viral infection.

80

81 Recent studies have emphasized the emerging role of the hexosamine biosynthesis  
82 pathway (HBP)—a branch of glucose metabolism—in host innate immunity. HBP links  
83 cellular glucose, glutamine, acetyl-CoA, and uridine triphosphate (UTP) concentrations with  
84 signaling transduction (Hanover *et al*, 2012). Approximately 2–5% of the total glucose  
85 entering a cell is converted to uridine diphosphate N-acetylglucosamine (UDP-GlcNAc)  
86 (McClain & Crook, 1996)—the end-product of HBP—and serves as a donor for O-linked  
87  $\beta$ -N-acetylglucosamine (O-GlcNAc) modification (also known as O-GlcNAcylation) (Torres &  
88 Hart, 1984). O-GlcNAc transferase (OGT) and O-GlcNAcase (OGA) are responsible for the  
89 addition and removal of N-acetylglucosamine (GlcNAc) from Ser and Thr residues of target  
90 proteins. Several key host proteins involved in immune modulation, including signal  
91 transducer and activator of transcription-3 (STAT3), MAVS, and receptor-interacting  
92 serine/threonine-protein kinase 3 (RIPK3), are targets for O-GlcNAcylation (Li *et al*, 2017,  
93 2018, 2019a; Song *et al*, 2019). However, the mechanism by which HBP-mediated  
94 O-GlcNAc modifications enhance antiviral innate immunity remains to be fully understood.

95

96 Hepatitis B virus (HBV) infection causes liver diseases, including acute and chronic hepatitis,  
97 cirrhosis, and hepatocellular carcinoma, which is a major global public health concern (Tsai  
98 *et al*, 2018). Current therapies improve both the quality of life and survival of patients with  
99 hepatitis B. However, new therapeutic approaches are needed to achieve functional cure of  
100 HBV infection (Fanning *et al*, 2019).

101

102 In this study, we investigated metabolic responses of host cells to HBV infection.  
103 Our results show that HBP-mediated O-GlcNAcylation regulates the antiviral activity of  
104 SAMHD1. Moreover, OGT promotes O-GlcNAcylation on Ser93 to enhance SAMHD1  
105 stability and tetramerization, which is important for its antiviral activity. Our study established  
106 a link between HBP, O-GlcNAc modification, and antiviral innate immunity by targeting  
107 SAMHD1, thereby providing a potential drug target for treating HBV and human  
108 immunodeficiency virus-1 (HIV-1) infection.

109

## 110 **Results**

### 111 **HBV infection upregulates GLUT1 expression and enhances HBP activity and protein**

#### 112 **O-GlcNAcylation**

113 To explore metabolic changes in response to HBV infection, a metabolomics assay was  
114 performed in AdHBV-1.3-infected HepG2 cells (HepG2-HBV1.3) and AdGFP-infected  
115 HepG2 cells (HepG2-GFP). Principal component analysis showed that HBV infection  
116 dramatically changes the intracellular metabolic profile of HepG2 cells (Fig. 1A). Several  
117 metabolic pathways, including central carbon metabolism, amino sugar and nucleotide  
118 sugar metabolism (Supplementary Fig. 1A) were significantly affected. Recent studies have  
119 shown that glucose metabolism plays a key role in host antiviral immunity (Li *et al*, 2018;  
120 Song *et al*, 2019). Hence, we determined the effect of altering glucose metabolism in  
121 HepG2-HBV1.3 cells. The expression level of several intermediate metabolites in glucose  
122 metabolism, including 3-phospho-glycerate, GlcNAc, N-acetyl glucosamine 6- phosphate  
123 (GlcNAc-6-P), and UDP-GlcNAc-the end-product of HBP-was increased upon HBV infection  
124 (Fig. 1B-D). To confirm this result, we established a strain of HepG2 cells engineered to  
125 express the human solute carrier family 10 member 1 (*SLC10A1*, also called NTCP) gene  
126 (HepG2-NTCP cells), which allows them susceptible to HBV infection (Hu *et al*, 2019).  
127 Targeted liquid chromatography-tandem mass spectrometry (LC-MS/MS) results showed a  
128 significant increase in UDP-GlcNAc and glucose levels in HBV-infected HepG2-NTCP,  
129 stable HBV-expressing HepAD38 (a tetracycline (Tet) inducible HBV expression cell line)  
130 (Fig. 1E-F), and AdHBV-1.3-infected HepG2 (Supplementary Fig. 1B-1C) cells. These results  
131 were consistent with those observed in HepG2.2.15, an HBV-replicating cell line (Li *et al*,  
132 2015). Because OGT-mediated protein O-GlcNAcylation is highly dependent on the  
133 intracellular concentration of the donor substrate UDP-GlcNAc, we examined whether HBV  
134 infection can affect O-GlcNAc modification in host cells. Total protein O-GlcNAcylation in

135 HBV-infected HepG2-NTCP cells significantly increased 6 to 9 days post HBV infection. A  
136 similar result was observed in HepAD38 (Tet-off) cells (3 to 7 days after Tet removal from  
137 the medium) (Fig. 1G). Further, GLUT1 expression was markedly enhanced in our HBV cell  
138 models (Fig. 1H-I and Supplementary Fig.1D-E). Elevated glucose levels can increase HBP  
139 flux and enhance UDP-GlcNAc synthesis (Housley *et al*, 2008). However, we did not  
140 observe significant changes in the protein levels of OGT, OGA, and GFPT1—the key  
141 enzymes that regulate HBP flux and protein O-GlcNAcylation (Supplementary  
142 Fig.1F-G). These findings demonstrate that HBV infection upregulates GLUT1 expression,  
143 promotes glucose uptake, and increases UDP-GlcNAc synthesis and protein  
144 O-GlcNAcylation in host cells.

145

#### 146 **Inhibition of protein O-GlcNAcylation promotes HBV replication in host cells**

147 Next, we evaluated the effects of protein O-GlcNAcylation on HBV replication. HBV-infected  
148 HepG2-NTCP cells, HepAD38 (Tet-off) cells, and AdHBV-1.3-infected HepG2 cells were  
149 treated with inhibitors of GLUT1, GFPT1, OGT, and OGA. Pharmacological inhibition of  
150 GLUT1, GFPT1, and OGT reduced total protein O-GlcNAcylation levels (Fig. 2A-C,  
151 Supplementary Fig. 2A-C and Supplementary Fig. 3A-C), and promoted HBV replication (Fig.  
152 2D-I, Supplementary Fig. 2D-F and Supplementary Fig. 3D-F). Conversely, pharmacological  
153 inhibition of OGA increased protein O-GlcNAcylation levels (Fig. 2J, Supplementary Fig. 2G  
154 and Supplementary Fig. 3G) but suppressed HBV replication (Fig. 2K-L, Supplementary Fig.  
155 2H and Supplementary Fig. 3H). These data suggest that HBP-mediated O-GlcNAcylation  
156 positively regulates host antiviral immune response against HBV. The results of  
157 pharmacological inhibitor studies were similar to those obtained from shRNA-mediated  
158 knockdown of *GLUT1*, *GFPT*, *OGT*, or *OGA* in HepAD38 (Tet-off), HBV-infected  
159 HepG2-NTCP, and AdHBV-1.3-infected HepG2 cells (Fig. 3 and Supplementary Fig. 4).

160 Taken together, these results indicate that inhibition of HBP or protein O-GlcNAcylation  
161 promotes HBV replication, whereas increased O-GlcNAc modifications can enhance host  
162 antiviral innate immune response against HBV.

163

#### 164 **OGT mediates O-GlcNAcylation of SAMHD1 upon HBV infection**

165 To further investigate the mechanism by which OGT-mediated protein O-GlcNAcylation  
166 promotes host antiviral innate immunity during HBV infection, we screened putative  
167 O-GlcNAc-modified proteins in HepAD38 (Tet-off) cells using the immunoprecipitation assay  
168 coupled with mass spectrometry (IP-MS). Cell lysates were immunoprecipitated with  
169 O-GlcNAc antibodies and analyzed by LC-MS/MS. A total of 1,034 candidate  
170 O-GlcNAc-modified proteins were identified (Supplementary Table 1). Gene ontology  
171 analysis showed that several proteins were involved in innate immune and inflammatory  
172 responses (Supplementary Fig. 5A). We next focused on SAMHD1, which plays an  
173 important role in promoting host antiviral innate immunity (Ballana & Esté, 2015).  
174 Interactions between OGT and SAMHD1 were demonstrated by co-immunoprecipitation  
175 (co-IP) experiments in HepG2 cells (Fig. 4A-B). Confocal analysis indicated that OGT and  
176 SAMHD1 are co-localized in the nucleus (Fig. 4C). We subsequently constructed three  
177 SAMHD1 deletion mutants (Fig. 4D) and showed that the SAM domain of SAMHD1 is  
178 required for its interaction with OGT (Fig. 4E). Immunoprecipitated Flag-tagged SAMHD1  
179 exhibited a strong O-GlcNAc modification signal in HEK293 cells upon treatment with the  
180 OGA inhibitor PUGNAc (Fig. 4F). Meanwhile, HBV replication enhanced SAMHD1  
181 O-GlcNAcylation in HepAD38 (Tet-off) cells (Fig. 4G) and HBV-infected HepG2-NTCP cells  
182 (Supplementary Fig. 5B). These results were further confirmed by affinity chromatography  
183 using the succinylated wheat germ agglutinin (sWGA), a modified lectin that specifically



184 binds O-GlcNAc-containing proteins (Fig. 4H-I). Collectively, these data indicate that  
185 SAMHD1 interacts with and can be O-GlcNAcylated by OGT upon HBV infection.

186

### 187 **OGT-mediated O-GlcNAcylation on Ser93 enhances SAMHD1 stability**

188 Next, we sought to map the O-GlcNAcylation site(s) on SAMHD1. Flag-tagged SAMHD1  
189 was purified from HepG2-HBV1.3 cells and analyzed by MS. As shown in Fig. 4J, SAMHD1  
190 was O-GlcNAcylated on Ser93 (S93). Interestingly, SAMHD1 S93 is well conserved among  
191 mammalian species (Fig. 4K). We then generated site-specific point mutants of SAMHD1.  
192 Mutation of S93 with Ala (S93A) largely reduced O-GlcNAc signal (Fig. 4L-M, and  
193 Supplementary Fig. 5C). To further examine the effect of O-GlcNAcylation on SAMHD1  
194 stability, Flag-tagged wild-type or S93A mutant SAMHD1 was overexpressed alone or with  
195 shOGT in HepAD38 cells. The stability of exogenous SAMHD1 was decreased upon the  
196 expression of shOGT or S93A mutant (Fig. 5A-D). Moreover, SAMHD1 stability and  
197 ubiquitination was increased upon HBV infection (Fig. 5A-E). Furthermore, the  
198 administration of PUGNAC dramatically suppressed total and K48-linked ubiquitination of  
199 wild-type SAMHD1 (Fig. 5F); however, the effect on S93A ubiquitination was minimal (Fig.  
200 5G). The S93A mutant was more ubiquitinated than wild-type SAMHD1 (Fig. 5G). These  
201 data indicate that O-GlcNAcylation of SAMDH1 at Ser93 stabilizes SAMHD1 by preventing  
202 its ubiquitination.

203

### 204 **O-GlcNAcylation of SAMHD1 on Ser93 enhances its antiviral activity**

205 It is known that the tetramer conformation of SAMHD1 is required for its dNTP  
206 triphosphohydrolase (dNTPase) activity (Yan *et al*, 2013). Herein, we sought to determine  
207 whether the S93A mutant affects SAMHD1 tetramerization and dNTPase activity.

208 Recombinant WT and S93A SAMHD1 were expressed and purified (Supplementary Fig.

209 6A-B). We found that S93A mutation destabilized SAMDH1 tetramers in HepAD38 cells (Fig.  
210 6A) and reduced its dNTPase activity *in vitro* (Supplementary Fig. 6C-D). To test the effect of  
211 S93 O-GlcNAcylation on SAMHD1 antiviral activity, we deleted endogenous SAMHD1 in our  
212 HBV cell models and THP-1 cells using CRISPR-Cas9-mediated gene editing, and  
213 transfected wild-type or SAMHD1 variants into SAMHD1-knockout HepAD38 (Tet-off) (Fig.  
214 6B), AdHBV-1.3-infected HepG2 (Fig. 6C), and HepG2-NTCP cells. A phospho-mimetic  
215 mutation (T592E) was used as a control that also decreased SAMHD1 dNTPase activity and  
216 abrogated its antiviral activity (Sommer *et al*, 2016). Both southern blotting (Fig. 6B-C) and  
217 qPCR (Fig. 6D-F) results indicated that S93A mutation impairs the ability of SAMHD1 to  
218 inhibit HBV replication *in vitro*. A previous study showed that SAMHD1 dNTPase activity is  
219 essential for HIV-1 restriction (Hansen *et al*, 2014). Therefore, we investigated the effect of  
220 SAMHD1 O-GlcNAcylation on HIV-1 infection. THP-1 cells were infected with a vesicular  
221 stomatitis virus G (VSV-G) protein pseudotyped HIV-1 molecular clone carrying the  
222 luciferase gene reporter, and virus replication was assessed by quantifying luciferase activity.  
223 Our results showed that protein O-GlcNAcylation was increased upon HIV-1 infection in  
224 THP-1 cells (Fig. 6G). Subsequently, wild-type or SAMHD1 variants were transfected into  
225 SAMHD1-KO THP-1 cells. S93A mutation also impaired the ability of SAMHD1 to restrict  
226 HIV-1 replication in this single-round HIV-1 infection model (Fig. 6H). Treatment of cells with  
227 the GFPT inhibitor 6-diazo-5-oxo-L-norleucine (DON) and the OGT inhibitor ST045849  
228 significantly increased luciferase activity, whereas treatment with the OGA inhibitor PUGNAc  
229 reduced luciferase activity (Fig. 6I). Taken together, these results indicate that  
230 O-GlcNAcylation of SAMHD1 S93 promotes its antiviral activity *in vitro*.

231

232 **HBV infection promotes UDP-GlcNAc biosynthesis and O-GlcNAcylation *in vivo***

233 We used an HBV-transgenic (HBV-Tg) mouse model to verify our results *in vivo*  
234 (Fig.7A).The level of O-GlcNAcylation was significantly higher in the liver tissues of HBV-Tg  
235 mice than in those of normal C57BL/6 mice (Fig. 7B). Consistent with our *in vitro* data, the  
236 administration of DON significantly reduced UDP-GlcNAc levels (Fig. 7C) and stimulated  
237 HBV replication (Fig. 7D-F) in the mouse model of HBV infection, whereas the administration  
238 of Thiamet G decreased serum HBV DNA (Fig. 7E), liver HBcAg (Fig. 7F) and HBV DNA  
239 (Fig. 7G) levels in mice. Protein O-GlcNAcylation levels in the liver tissues of HBV-Tg mice  
240 were increased upon Thiamet G administration, but decreased upon DON administration  
241 (Fig. 7H). These results indicate that Thiamet G can promote host antiviral immunity by  
242 increasing protein O-GlcNAcylation.Finally, we examined UDP-GlcNAc biosynthesis and  
243 O-GlcNAcylation levels in patients with chronic hepatitis B (CHB). The levels of serum  
244 UDP-GlcNAc (Fig. 7I), GLUT1 protein (Fig. 7J), and total O-GlcNAcylation (Fig. 7J and 7K)  
245 were markedly higher in the liver tissues of patients with CHB than in those of normal  
246 controls. In addition, SAMHD1 O-GlcNAcylation was significantly increased in the liver  
247 tissues of the patients with CHB (Fig. 7K). Overall, our study suggests that HBV infection  
248 upregulates GLUT1 expression and increases UDP-GlcNAc biosynthesis and  
249 O-GlcNAcylation *in vivo*. As an essential O-GlcNAcyated protein, SAMHD1 can exert its  
250 antiviral activity and elicit a robust host innate immune response against HBV infection.

251

252

253 **Discussion**

254 Although previous studies have demonstrated that HBV infection can alter glucose  
255 metabolism in host cells, the role and underlying mechanisms of metabolic regulation of  
256 antiviral immune responses remain elusive. In this study, we demonstrate that HBV  
257 increases GLUT1 expression on hepatocyte surface, thereby facilitating glucose uptake.  
258 This enhanced nutrient state consequently provides substrates to HBP to produce  
259 UDP-GlcNAc, leading to an increase in protein O-GlcNAcylation. Importantly, we found that  
260 pharmacological or transcriptional inhibition of HBP and O-GlcNAcylation can promote HBV  
261 replication. Furthermore, we showed that OGT-mediated O-GlcNAcylation of SAMHD1 on  
262 Ser93 is critical for its antiviral activity. Our results therefore indicate that O-GlcNAcylation  
263 can positively regulate host antiviral immune response against HBV infection.

264

265 Similar to the metabolic reprogramming in proliferating cancer cells, virus reprogram host  
266 cell metabolism. It has been reported that several viruses increase glucose consumption  
267 and reprogram glucose metabolism in the host cell (Purdy & Luftig, 2019; Thaker *et al*, 2019).  
268 GLUT1 expression was increased in host cells infected with HIV-1 (Loisel-Meyer *et al*, 2012;  
269 Palmer *et al*, 2014), Kaposi's sarcoma-associated herpes virus (Gonnella *et al*, 2013),  
270 dengue virus (Fontaine *et al*, 2015), and Epstein-Barr virus (Zhang *et al*, 2017). Our findings  
271 are consistent with previous transcriptome-wide analyses, which have also shown  
272 HBV-mediated upregulation of GLUT1 (Lamontagne *et al*, 2016). It has been suggested that  
273 HBV pre-S2 mutant increases GLUT1 expression via mammalian target of rapamycin  
274 signaling cascade, leading to enhanced glucose uptake (Teng *et al*, 2015, 2). However, the  
275 precise molecular mechanism by which HBV upregulates GLUT1 remains poorly  
276 understood.

277

278 The enhanced glucose uptake by glucose transporter not only accelerates glycolysis, but  
279 may also increase flux into branch pathways, such as the pentose phosphate pathway and  
280 HBP, which occur in cancer cells (Ma & Vosseller, 2014). Previous studies have reported  
281 that HBP plays an important role in host innate immunity. Consistent with the results of a  
282 previous study with HepG2.2.15 cells (Li *et al*, 2015), our results showed that HBV infection  
283 can promote HBP activity and increase UDP-GlcNAc levels in different cell models. Li *et al*.  
284 reported that enhanced HBP activity is essential for HBV replication because  
285 pharmacological or transcription suppression of *GFPT1* inhibits HBV replication in  
286 HepG2.2.15 cells. However, they did not use an *in vivo* HBV model to study the underlying  
287 mechanism. In contrast, we showed that blockade of HBP promotes HBV replication,  
288 whereas stimulation of HBP significantly suppresses HBV replication both *in vitro* and *in vivo*.  
289 In addition, we observed similar results upon HIV-1 infection using a single-round infection  
290 model. Although we could not exclude the possibility that differences between HBV cell  
291 models cause this discrepancy, our results show that increased HBP flux and  
292 hyper-O-GlcNAcylation can upregulate host antiviral innate response. Several other studies  
293 have reported that HBP and/or protein O-GlcNAcylation promotes host antiviral immunity  
294 against RNA viruses, including VSV (Li *et al*, 2018), influenza virus (Song *et al*, 2019), and  
295 hepatitis C virus (Herzog *et al*, 2019). Thus, the present study confirms and expands our  
296 current understanding of the antiviral activity of HBP and protein O-GlcNAcylation upon DNA  
297 virus infection, which is similar to its antiviral activity upon infection by certain RNA viruses.  
298  
299 By characterizing the role of protein O-GlcNAcylation during HBV replication, we uncovered  
300 SAMHD1 as an important target of OGT and established a link between O-GlcNAcylation  
301 and antiviral immune response against HBV infection. SAMHD1, an effector of innate  
302 immunity, can restrict most retroviruses (such as HIV-1) and several DNA viruses (including

303 HBV) by depleting the intracellular pool of dNTPs (Ballana & Esté, 2015). Several  
304 post-translational modifications, including phosphorylation (White *et al*, 2013, 1) and  
305 ubiquitination (Li *et al*, 2019b) have been reported to be critical for SAMHD1 function. Herein,  
306 we identified Ser93 as a key O-GlcNAcylation site on SAMHD1 using LC-MS/MS.  
307 Importantly, loss of O-GlcNAcylation by S93A mutation increased K48-linked ubiquitination,  
308 thus decreased the stability and dNTPase activity of SAMHD1, suggesting that  
309 O-GlcNAcylation promotes the antiviral activity of SAMHD1.

310

311 Because these results demonstrated the importance of protein O-GlcNAcylation in host  
312 antiviral innate immunity against HBV, we proposed that an increase in SAMHD1  
313 O-GlcNAcylation by inhibiting OGA activity could be used as a potential antiviral strategy.  
314 This is in line with recent results indicating that increased MAVS O-GlcNAcylation is  
315 essential to activate host innate immunity against RNA viruses (Li *et al*, 2018; Song *et al*,  
316 2019). However, hyper-O-GlcNAcylation has been reported to stabilize several oncogenic  
317 factors in several cancers associated with oncogenic virus infection (Makwana *et al*, 2019).  
318 Human papillomavirus 16 E6 protein can upregulate OGT and stabilize c-MYC via  
319 O-GlcNAcylation, thus promoting HPV-induced carcinogenesis (Zeng *et al*, 2016). Herzog *et*  
320 *al.* demonstrated that protein O-GlcNAcylation is involved in HCV-induced disease  
321 progression and carcinogenesis (Herzog *et al*, 2019). Thus, the role of protein  
322 O-GlcNAcylation in HBV pathogenesis and the antiviral response through enhanced protein  
323 O-GlcNAcylation remain to be further studied.

324

325 In conclusion, we uncovered a link between metabolic reprogramming and antiviral innate  
326 immunity against HBV infection. We demonstrated that HBV infection upregulates GLUT1  
327 expression and promotes HBP flux *in vitro* and *in vivo*. In addition, increased UDP-GlcNAc

328 biosynthesis and hyper-O-GlcNAcylation can enhance host antiviral innate response.  
329 Mechanistically, OGT-mediated O-GlcNAcylation of SAMHD1 on Ser93 stabilizes SAMHD1  
330 and enhances its antiviral activity (Fig. 7I). This study broadens our understanding of  
331 SAMHD1 post-translational modification and provides new insights into the importance of  
332 HBP and protein O-GlcNAcylation in antiviral innate immunity.  
333

## 334 **Materials and Methods**

### 335 **Animal models**

336 HBV-transgenic (HBV-Tg) mice (n = 6 for each group) were kindly provided by Prof.  
337 Ning-shao Xia, School of Public Health, Xiamen University(Huang *et al*, 2006). C57BL/6J  
338 mice (6- to-8-week-old, six per group) were provided by the Laboratory Animal Center of  
339 Chongqing Medical University (SCXK (YU) 2018-0003). Mice were intraperitoneally injected  
340 with Don (1 mg/kg body weight), Thiamet G (20 mg/kg body weight), or PBS (control) every  
341 other day for 10 times. On day 20 post-administration, mouse serum and liver tissue  
342 specimens were collected for real-time PCR, southern blotting, and immunohistochemical  
343 staining. Mice were treated in accordance with the guidelines established by the Institutional  
344 Animal Care and Use Committee at the Laboratory Animal Center of Chongqing Medical  
345 University. The animal care and use protocols adhered to the National Regulations for the  
346 Administration of Laboratory Animals to ensure minimal suffering.

347

### 348 **Samples from patients with chronic hepatitis B virus infection**

349 The study protocol was approved by the Medical Ethics Committee of Chongqing Medical  
350 University. Informed consent was obtained from patients who met the inclusion criteria for  
351 chronic HBV infection.

352

### 353 **Metabolites analysis**

354 To extract metabolites from quenched serum/plasma samples or cell culture supernatants,  
355 400  $\mu$ L chilled methanol: acetonitrile (2:2, v/v) was added to 100  $\mu$ L of each sample. The  
356 mixture was vortexed three times for 1 min each with 5-min incubation at 4°C after each  
357 vortexing step. After the final vortexing step of 30 s, the mixture was incubated on ice for 10  
358 min. Thereafter, 100  $\mu$ L chilled HPLC-certified water was added to the samples, mixed for 1



359 min, and centrifuged at 13,000g for 10 min at 4°C. Finally, the liquid phase (supernatant) of  
360 each sample was transferred into a new tube for UHPLC-QTOF-MS analysis in Shanghai  
361 Applied Protein Technology Co., Ltd. UDP-GlcNAc and glucose were quantified using  
362 targeted liquid chromatography-tandem mass spectrometry (LC-MS/MS). The data  
363 acquisition, principal component analysis, heatmap and pathway impact analysis were  
364 performed by Shanghai Applied Protein Technology Co., Ltd.

365

### 366 **Immunoprecipitation assay coupled with mass spectrometry (IP-MS)**

367 HepAD38 (Tet-off) cell lysates were incubated overnight with an anti-O-GlcNAc antibody at  
368 4°C, followed by a 4-h incubation with protein A/G agarose beads. Immunoprecipitated  
369 complexes were eluted and stained with Coomassie blue. Stained protein bands were sent  
370 to Shanghai Applied Protein Technology Co., Ltd for identification of potential  
371 O-GlcNAc-modified proteins. Protein bands were dissolved in 1 mL chilled methanol:  
372 acetonitrile: H<sub>2</sub>O (2:2:1, v/v/v) and sonicated at low temperature (30 min); this process was  
373 repeated twice. The supernatant was dried in a vacuum centrifuge. For LC-MS analysis,  
374 samples were re-dissolved in 100 µL acetonitrile: water (1:1, v/v). Sample analyses were  
375 performed using a UHPLC system (1290 Infinity LC, Agilent Technologies) coupled to a  
376 quadrupole time-of-flight analyzer (AB Sciex Triple TOF6600) at Shanghai Applied Protein  
377 Technology Co., Ltd.

378

### 379 **SAMHD1 O-GlcNAcylation site mapping**

380 Mass spectrometry was performed to identify SAMHD1 O-GlcNAcylation sites, as described  
381 previously (Peng *et al*, 2017). Briefly, immunoprecipitated SAMHD1 from HEK293T cells  
382 was subjected to SDS-PAGE. The band corresponding to SAMHD1 was excised, digested  
383 overnight with trypsin, and subjected to liquid chromatography-tandem mass spectrometry

384 (LC-MS/MS) analysis. An online LC-MS/MS setup consisting of an Easy-nLC system and an  
385 Orbitrap Fusion Lumos Tribrid mass spectrometer (Thermo Scientific, Germany) equipped  
386 with a nanoelectrospray ion source was used for all LC-MS/MS experiments. Raw MS files  
387 were searched against the UniProt database using MaxQuant software (version 1.5.2.8).  
388 The fixed modification was set to C (carbamidomethyl) and the variable modifications were  
389 set to M (oxidation), protein N-term (acetyl), and S/T (O-GlcNAc). The peptide tolerance for  
390 the first search was set at 20 ppm and that for the main search was set at 6 ppm. The  
391 MS/MS tolerance was 0.02 Da. The false discovery level in PSM and protein was 1%. The  
392 match between runs was used and the minimum score for modified peptides was set at 40.

393

#### 394 **Statistical Analysis**

395 All data are expressed as the mean  $\pm$  standard deviation (SD). All statistical analyses were  
396 performed using GraphPad Prism 5.0 software (GraphPad Software Inc.). Statistical  
397 significance was determined using one-way ANOVA for multiple comparisons. Student's  
398 *t*-test was used to compare two groups.  $P < 0.05$  was considered statistically significant.

399

400 For detailed descriptions of other methods, please refer to **Supplementary Methods**.

401

402

403 **Acknowledgements**

404 We are grateful to Dr. T.-C He (University of Chicago, USA) for providing the pAdEasy  
405 plasmid. We thank Prof. Bing Sun (Shanghai Institute of Biochemistry and Cell Biology,  
406 China) for providing the pLL3.7 vector. We also thank Prof. Cheguo Cai (Wuhan University,  
407 China) for providing the pNL4-3.Luc.R-E- plasmid. This work was supported by National  
408 Natural Science Foundation of China (grant nos. 81872270, 81572683, 81661148057), the  
409 Natural Science Foundation Project of Chongqing (cstc2018jcyjAX0254,  
410 cstc2019jcyj-msxmX0587), the Major National S&T program (2017ZX10202203-004), the  
411 National Key Research and Development Program of China (2018YFE0107500), the  
412 Leading Talent Program of CQ CSTC (CSTCCXLJRC201719), and the Scientific Research  
413 Innovation Project for Postgraduate in Chongqing (grant nos CYB19168, CYS19193)

414

415 **Authors Contributions**

416 NT, AH, and KW conceived the study and designed the experiments. JH, QG, YY and XJ  
417 performed most experiments and analyzed the data. WZ and LC performed SAMHD1  
418 O-GlcNAcylation site mapping. YC and ZZ collected clinical samples. LL generated  
419 SAMHD1 mutants. QL assisted with HepG2-NTCP cell culture. YH, HZ and XL provided  
420 guidance and advice. JH, QG, KW, and NT wrote the manuscript with all authors providing  
421 feedback.

422

423 **Declaration of Interest**

424 The authors declare no competing interests.

425

426 **References**

- 427 Ballana E & Esté JA (2015) SAMHD1: At the Crossroads of Cell Proliferation, Immune  
428 Responses, and Virus Restriction. *Trends Microbiol.* **23**: 680–692
- 429 Chang C-H, Curtis JD, Maggi LB, Faubert B, Villarino AV, O'Sullivan D, Huang SC-C,  
430 van der Windt GJW, Blagih J, Qiu J, Weber JD, Pearce EJ, Jones RG & Pearce EL  
431 (2013) Posttranscriptional Control of T Cell Effector Function by Aerobic Glycolysis.  
432 *Cell* **153**: 1239–1251
- 433 Fanning GC, Zoulim F, Hou J & Bertoletti A (2019) Therapeutic strategies for hepatitis B  
434 virus infection: towards a cure. *Nat. Rev. Drug Discov.* Available at:  
435 <http://www.nature.com/articles/s41573-019-0037-0> [Accessed August 29, 2019]
- 436 Fontaine KA, Sanchez EL, Camarda R & Lagunoff M (2015) Dengue Virus Induces and  
437 Requires Glycolysis for Optimal Replication. *J. Virol.* **89**: 2358–2366
- 438 Gonnella R, Santarelli R, Farina A, Granato M, D'Orazi G, Faggioni A & Cirone M (2013)  
439 Kaposi sarcoma associated herpesvirus (KSHV) induces AKT hyperphosphorylation,  
440 bortezomib-resistance and GLUT-1 plasma membrane exposure in THP-1 monocytic  
441 cell line. *J. Exp. Clin. Cancer Res.* **32**: 79
- 442 Hanover JA, Krause MW & Love DC (2012) linking metabolism to epigenetics through  
443 O-GlcNAcylation: Bittersweet memories. *Nat. Rev. Mol. Cell Biol.* **13**: 312–321
- 444 Hansen EC, Seamon KJ, Cravens SL & Stivers JT (2014) GTP activator and dNTP  
445 substrates of HIV-1 restriction factor SAMHD1 generate a long-lived activated state.  
446 *Proc. Natl. Acad. Sci.* **111**: E1843–E1851
- 447 Haskó G & Cronstein BN (2004) Adenosine: an endogenous regulator of innate immunity.  
448 *Trends Immunol.* **25**: 33–39
- 449 Herzog K, Bandiera S, Pernot S, Fauvelle C, Jühling F, Weiss A, Bull A, Durand SC,  
450 Chane-Woon-Ming B, Pfeffer S, Mercey M, Lerat H, Meunier J-C, Raffelsberger W,  
451 Brino L, Baumert TF & Zeisel MB (2019) Functional microRNA screen uncovers  
452 O-linked N-acetylglucosamine transferase as a host factor modulating hepatitis C  
453 virus morphogenesis and infectivity. *Gut*: gutjnl-2018-317423
- 454 Housley MP, Rodgers JT, Udeshi ND, Kelly TJ, Shabanowitz J, Hunt DF, Puigserver P & Hart  
455 GW (2008) O-GlcNAc Regulates FoxO Activation in Response to Glucose. *J. Biol.*  
456 *Chem.* **283**: 16283–16292
- 457 Hu J, Lin Y-Y, Chen P-J, Watashi K & Wakita T (2019) Cell and Animal Models for Studying  
458 Hepatitis B Virus Infection and Drug Development. *Gastroenterology* **156**: 338–354
- 459 Huang L-R, Wu H-L, Chen P-J & Chen D-S (2006) An immunocompetent mouse model for  
460 the tolerance of human chronic hepatitis B virus infection. *Proc. Natl. Acad. Sci.* **103**:  
461 17862–17867
- 462 Jung J, Zeng H & Horng T (2019) Metabolism as a guiding force for immunity. *Nat. Cell Biol.*  
463 **21**: 85–93

- 464 Lamontagne J, Mell JC & Bouchard MJ (2016) Transcriptome-Wide Analysis of Hepatitis B  
465 Virus-Mediated Changes to Normal Hepatocyte Gene Expression. *PLOS Pathog.* **12**:  
466 e1005438
- 467 Li H, Zhu W, Zhang L, Lei H, Wu X, Guo L, Chen X, Wang Y & Tang H (2015) The metabolic  
468 responses to hepatitis B virus infection shed new light on pathogenesis and targets  
469 for treatment. *Sci. Rep.* **5**
- 470 Li T, Li X, Attri KS, Liu C, Li L, Herring LE, Asara JM, Lei YL, Singh PK, Gao C & Wen H  
471 (2018) O-GlcNAc Transferase Links Glucose Metabolism to MAVS-Mediated Antiviral  
472 Innate Immunity. *Cell Host Microbe* **24**: 791-803.e6
- 473 Li X, Gong W, Wang H, Li T, Attri KS, Lewis RE, Kalil AC, Bhinderwala F, Powers R, Yin G,  
474 Herring LE, Asara JM, Lei YL, Yang X, Rodriguez DA, Yang M, Green DR, Singh PK  
475 & Wen H (2019a) O-GlcNAc Transferase Suppresses Inflammation and Necroptosis  
476 by Targeting Receptor-Interacting Serine/Threonine-Protein Kinase 3. *Immunity* **50**:  
477 576-590.e6
- 478 Li X, Zhang Z, Li L, Gong W, Lazenby AJ, Swanson BJ, Herring LE, Asara JM, Singer JD &  
479 Wen H (2017) Myeloid-derived cullin 3 promotes STAT3 phosphorylation by inhibiting  
480 OGT expression and protects against intestinal inflammation. *J. Exp. Med.* **214**:  
481 1093–1109
- 482 Li Z, Huan C, Wang H, Liu Y, Liu X, Su X, Yu J, Zhao Z, Yu X-F, Zheng B & Zhang W (2019b)  
483 TRIM21-mediated proteasomal degradation of SAMHD1 regulates its antiviral activity.  
484 *EMBO Rep.* **n/a**: e47528
- 485 Loisel-Meyer S, Swainson L, Craveiro M, Oburoglu L, Mongellaz C, Costa C, Martinez M,  
486 Cosset F-L, Battini J-L, Herzenberg LA, Herzenberg LA, Atkuri KR, Sitbon M, Kinet S,  
487 Verhoeyen E & Taylor N (2012) Glut1-mediated glucose transport regulates HIV  
488 infection. *Proc. Natl. Acad. Sci.* **109**: 2549–2554
- 489 Ma Z & Vosseller K (2014) Cancer Metabolism and Elevated O-GlcNAc in Oncogenic  
490 Signaling. *J. Biol. Chem.* **289**: 34457–34465
- 491 Makwana V, Ryan P, Patel B, Dukie S-A & Rudrawar S (2019) Essential role of  
492 O-GlcNAcylation in stabilization of oncogenic factors. *Biochim. Biophys. Acta BBA -*  
493 *Gen. Subj.* **1863**: 1302–1317
- 494 McClain DA & Crook ED (1996) Hexosamines and insulin resistance. *Diabetes* **45**:  
495 1003–1009
- 496 Mills EL, Ryan DG, Prag HA, Dikovskaya D, Menon D, Zaslona Z, Jedrychowski MP, Costa  
497 ASH, Higgins M, Hams E, Szpyt J, Runtsch MC, King MS, McGouran JF, Fischer R,  
498 Kessler BM, McGettrick AF, Hughes MM, Carroll RG, Booty LM, et al (2018) Itaconate  
499 is an anti-inflammatory metabolite that activates Nrf2 via alkylation of KEAP1. *Nature*  
500 **556**: 113–117
- 501 O'Neill LAJ & Artyomov MN (2019) Itaconate: the poster child of metabolic reprogramming in  
502 macrophage function. *Nat. Rev. Immunol.* **19**: 273–281
- 503 Palmer CS, Ostrowski M, Gouillou M, Tsai L, Yu D, Zhou J, Henstridge DC, Maisa A, Hearps

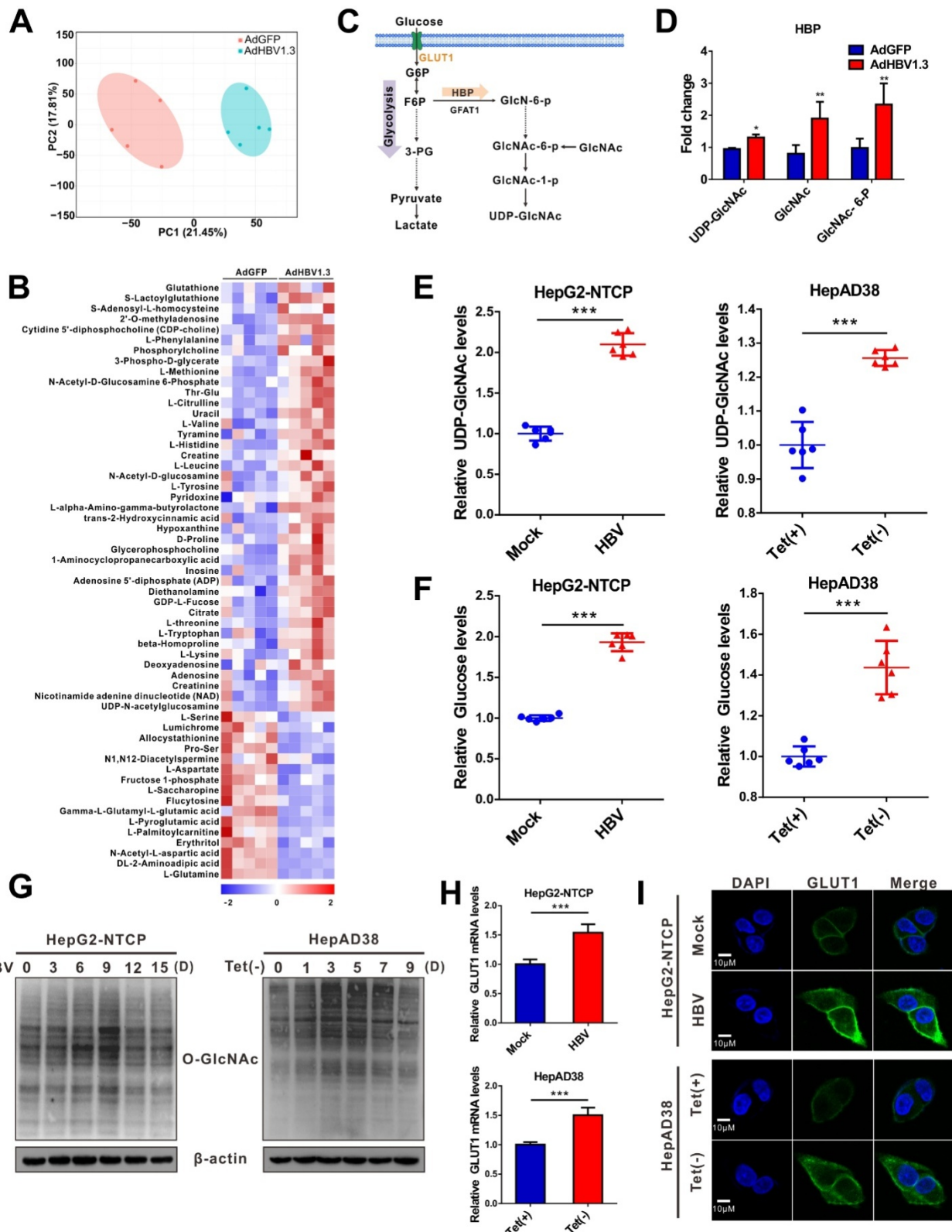
- 504 AC, Lewin SR, Landay A, Jaworowski A, McCune JM & Crowe SM (2014) Increased  
505 glucose metabolic activity is associated with CD4+ T-cell activation and depletion  
506 during chronic HIV infection. *AIDS Lond. Engl.* **28**: 297–309
- 507 Palsson-McDermott EM, Curtis AM, Goel G, Lauterbach MAR, Sheedy FJ, Gleeson LE,  
508 van den Bosch MWM, Quinn SR, Domingo-Fernandez R, Johnston DGW, Jiang J,  
509 Israelsen WJ, Keane J, Thomas C, Clish C, Vander Heiden M, Xavier RJ & O'Neill  
510 LAJ (2015) Pyruvate Kinase M2 Regulates Hif-1 $\alpha$  Activity and IL-1 $\beta$  Induction and Is  
511 a Critical Determinant of the Warburg Effect in LPS-Activated Macrophages. *Cell*  
512 *Metab.* **21**: 65–80
- 513 Peng C, Zhu Y, Zhang W, Liao Q, Chen Y, Zhao X, Guo Q, Shen P, Zhen B, Qian X, Yang D,  
514 Zhang J-S, Xiao D, Qin W & Pei H (2017) Regulation of the Hippo-YAP Pathway by  
515 Glucose Sensor O-GlcNAcylation. *Mol. Cell* **68**: 591-604.e5
- 516 Purdy JG & Luftig MA (2019) Reprogramming of cellular metabolic pathways by human  
517 oncogenic viruses. *Curr. Opin. Virol.* **39**: 60–69
- 518 Skelly AN, Sato Y, Kearney S & Honda K (2019) Mining the microbiota for microbial and  
519 metabolite-based immunotherapies. *Nat. Rev. Immunol.* **19**: 305–323
- 520 Sommer AFR, Rivière L, Qu B, Schott K, Riess M, Ni Y, Shepard C, Schnellbacher E,  
521 Finkernagel M, Himmelsbach K, Welzel K, Kettern N, Donnerhak C, Münk C, Flory E,  
522 Liese J, Kim B, Urban S & König R (2016) Restrictive influence of SAMHD1 on  
523 Hepatitis B Virus life cycle. *Sci. Rep.* **6**: 26616
- 524 Song N, Qi Q, Cao R, Qin B, Wang B, Wang Y, Zhao L, Li W, Du X, Liu F, Yan Y, Yi W, Jiang  
525 H, Li T, Zhou T, Li H, Xia Q, Zhang X, Zhong W, Li A, et al (2019) MAVS  
526 O-GlcNAcylation Is Essential for Host Antiviral Immunity against Lethal RNA Viruses.  
527 *Cell Rep.* **28**: 2386-2396.e5
- 528 Teng C-F, Hsieh W-C, Wu H-C, Lin Y-J, Tsai H-W, Huang W & Su I-J (2015) Hepatitis B Virus  
529 Pre-S2 Mutant Induces Aerobic Glycolysis through Mammalian Target of Rapamycin  
530 Signal Cascade. *PLoS ONE* **10**
- 531 Thaker SK, Ch'ng J & Christofk HR (2019) Viral hijacking of cellular metabolism. *BMC Biol.*  
532 **17**: 59
- 533 Torres CR & Hart GW (1984) Topography and polypeptide distribution of terminal  
534 N-acetylglucosamine residues on the surfaces of intact lymphocytes. Evidence for  
535 O-linked GlcNAc. *J. Biol. Chem.* **259**: 3308–3317
- 536 Tsai K-N, Kuo C-F & Ou J-HJ (2018) Mechanisms of Hepatitis B Virus Persistence. *Trends*  
537 *Microbiol.* **26**: 33–42
- 538 Tsalikis J, Croitoru DO, Philpott DJ & Girardin SE (2013) Nutrient sensing and metabolic  
539 stress pathways in innate immunity. *Cell. Microbiol.* **15**: 1632–1641
- 540 Vastag L, Koyuncu E, Grady SL, Shenk TE & Rabinowitz JD (2011) Divergent Effects of  
541 Human Cytomegalovirus and Herpes Simplex Virus-1 on Cellular Metabolism. *PLoS*  
542 *Pathog.* **7**: e1002124

- 543 White TE, Brandariz-Nuñez A, Valle-Casuso JC, Amie S, Nguyen LA, Kim B, Tuzova M &  
544 Diaz-Griffero F (2013) The Retroviral Restriction Ability of SAMHD1, but Not Its  
545 Deoxynucleotide Triphosphohydrolase Activity, Is Regulated by Phosphorylation. *Cell*  
546 *Host Microbe* **13**: 441–451
- 547 Yan J, Kaur S, DeLucia M, Hao C, Mehrens J, Wang C, Golczak M, Palczewski K,  
548 Gronenborn AM, Ahn J & Skowronski J (2013) Tetramerization of SAMHD1 Is  
549 Required for Biological Activity and Inhibition of HIV Infection. *J. Biol. Chem.* **288**:  
550 10406–10417
- 551 Yu Y, Maguire TG & Alwine JC (2014) ChREBP, a glucose-responsive transcriptional factor,  
552 enhances glucose metabolism to support biosynthesis in human  
553 cytomegalovirus-infected cells. *Proc. Natl. Acad. Sci.* **111**: 1951–1956
- 554 Zeng Q, Zhao R-X, Chen J, Li Y, Li X-D, Liu X-L, Zhang W-M, Quan C-S, Wang Y-S, Zhai  
555 Y-X, Wang J-W, Youssef M, Cui R, Liang J, Genovese N, Chow LT, Li Y-L & Xu Z-X  
556 (2016) O-linked GlcNAcylation elevated by HPV E6 mediates viral oncogenesis. *Proc.*  
557 *Natl. Acad. Sci.* **113**: 9333–9338
- 558 Zhang D, Tang Z, Huang H, Zhou G, Cui C, Weng Y, Liu W, Kim S, Lee S, Perez-Neut M,  
559 Ding J, Czyz D, Hu R, Ye Z, He M, Zheng YG, Shuman HA, Dai L, Ren B, Roeder RG,  
560 et al (2019a) Metabolic regulation of gene expression by histone lactylation. *Nature*  
561 **574**: 575–580
- 562 Zhang J, Jia L, Lin W, Yip YL, Lo KW, Lau VMY, Zhu D, Tsang CM, Zhou Y, Deng W, Lung  
563 HL, Lung ML, Cheung LM & Tsao SW (2017) Epstein-Barr Virus-Encoded Latent  
564 Membrane Protein 1 Upregulates Glucose Transporter 1 Transcription via the  
565 mTORC1/NF-κB Signaling Pathways. *J. Virol.* **91**: e02168-16
- 566 Zhang W, Wang G, Xu Z-G, Tu H, Hu F, Dai J, Chang Y, Chen Y, Lu Y, Zeng H, Cai Z, Han F,  
567 Xu C, Jin G, Sun L, Pan B-S, Lai S-W, Hsu C-C, Xu J, Chen Z-Z, et al (2019b) Lactate  
568 Is a Natural Suppressor of RLR Signaling by Targeting MAVS. *Cell* **178**: 176-189.e15

569

## 570 **Figures and Figure Legends**

## Figure 1



571

572 **Fig. 1. HBV infection promotes HBP and increases protein O-GlcNAcylation**

573 (A) Principal component analysis of metabolite profiles obtained using a metabolomics



574 assay in HepG2 cells infected with AdHBV1.3 or AdGFP for 72 h.

575 **(B)** Heatmap of differentially expressed metabolites subjected to identical treatment

576 conditions as in (a). n = 5.

577 **(C)** An overview of the hexosamine biosynthesis pathway (HBP).

578 **(D)** Fold changes in the expression of differentially expressed intermediate metabolites of

579 HBP. n = 5.

580 **(E-F)** Fold change in the expression of UDP-GlcNAc (E) and glucose (F) in HBV-infected

581 HepG2-NTCP cells and HepAD38 cells with tetracycline inducible (Tet-off) HBV expression

582 was determined using the LC-MS/MS targeted metabolomics assay. n = 6.

583 **(G)** Immunoblot of total O-GlcNAc from HepG2-NTCP and HepAD38 cells treated for the

584 indicated periods.

585 **(H-I)** qPCR quantification (H) and immunofluorescence staining (I) of GLUT1 in

586 HepG2-NTCP and HepAD38 cells, DAPI (blue) was used to counterstain nuclei, n = 9. Scale

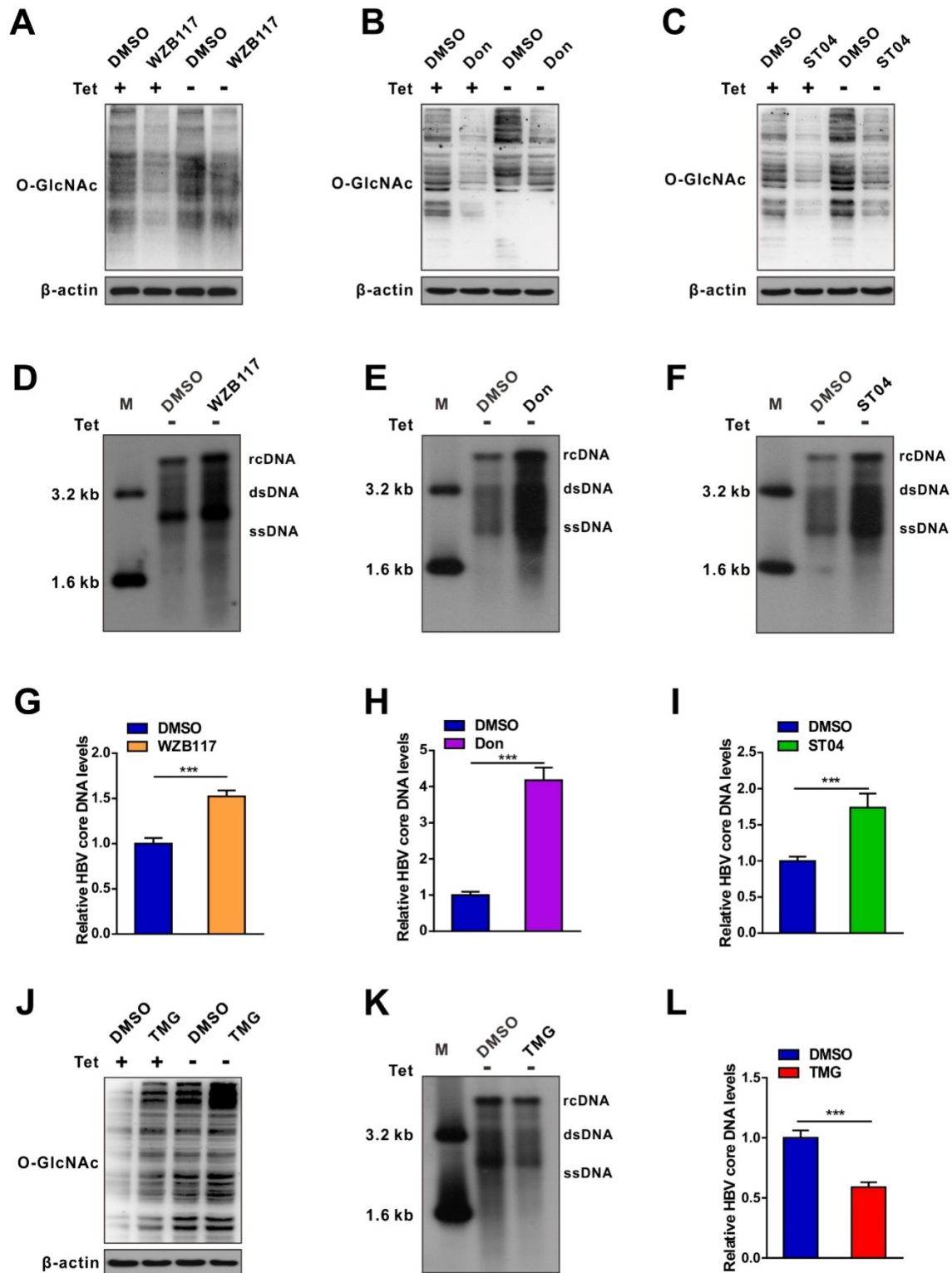
587 bar, 10  $\mu$ m.

588 Data are expressed as the mean  $\pm$  SD. *P* values were derived from unpaired, two-tailed

589 Student's *t*-test in E, F, and H; (\*\*\*) *P* < 0.001).

590

## Figure 2



591

592

**Fig. 2. Pharmacological inhibition of protein O-GlcNAcylation promotes HBV**

593

**replication**

594 **(A-C)** Immunoblot of total O-GlcNAc from tetracycline-inducible HepAD38 cells treated with  
595 or without GLUT1 inhibitor WZB117 (50  $\mu$ M) (A), GFPT1 inhibitor Don (30  $\mu$ M) (B), or OGT  
596 inhibitor ST04 (100  $\mu$ M) (C) for 72 h. Don, 6-Diazo-5-oxo-L-norleucine; ST04, ST045849.

597 **(D-F)** HBV DNA were detected by Southern blot assay in stable HBV-expressing HepAD38  
598 cells treated as above. rc DNA, relaxed circular DNA; ds DNA, double-stranded DNA; ss  
599 DNA, single-stranded DNA.

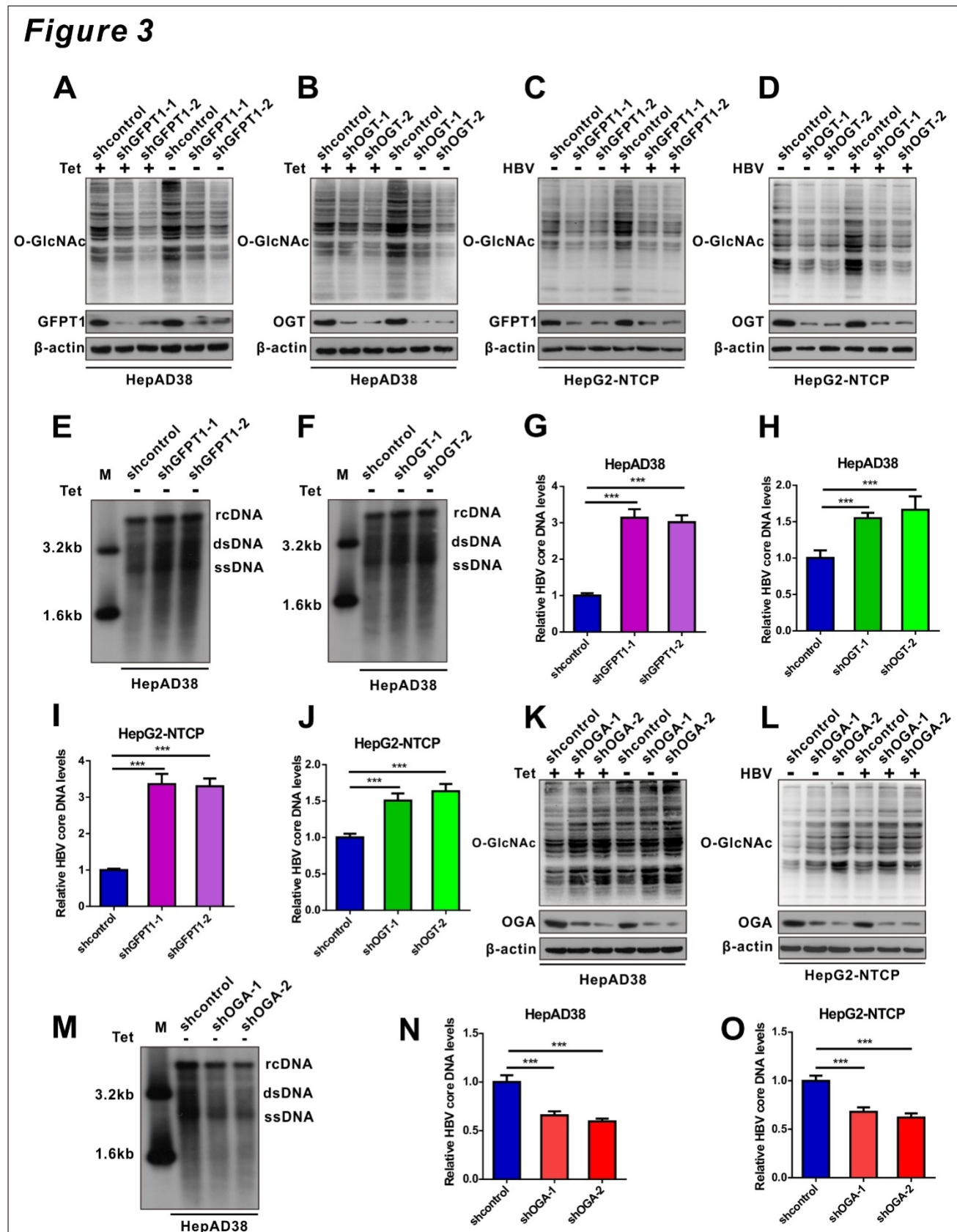
600 **(G-I)** Quantification of HBV core DNA levels in stable HBV-expressing HepAD38 cells  
601 treated as indicated using qPCR, n=9.

602 **(J)** Immunoblot of total O-GlcNAc from tetracycline-inducible HepAD38 cells treated with or  
603 without OGA inhibitor TMG (100  $\mu$ M) for 72 h. TMG, Thiamet G.

604 **(K-L)** Southern blot analysis of HBV DNA and qPCR quantification of HBV core DNA levels  
605 in stable HBV-expressing HepAD38 cells treated as in (J), n=9.

606 Data are expressed as the mean  $\pm$  SD. *P* values were derived from unpaired, two-tailed  
607 Student's *t*-test in G-I and L; (\*\*\*) *P* < 0.001).

608



609

610

**Fig. 3. shRNA-mediated inhibition of protein O-GlcNAcylation enhances HBV**

611

**replication**

612 **(A-D)** Immunoblot of total O-GlcNAc from tetracycline-inducible HepAD38 cells (A-B) and  
613 HBV-infected HepG2-NTCP cells (C-D) following shRNA-mediated knockdown of GFPT1  
614 and OGT.

615 **(E-H)** Southern blot analysis of HBV DNA (E-F) and qPCR quantification of HBV core DNA  
616 levels (G-H) in stable HBV-expressing HepAD38 cells treated as above, n=9.

617 **(I-J)** Quantification of HBV core DNA levels in HBV-infected HepG2-NTCP cells treated as  
618 indicated using qPCR, n=9.

619 **(K-L)** Immunoblot of total O-GlcNAc from OGA-knockdown HepAD38 (Tet-off) cells (K) and  
620 OGA-knockdown HBV-infected HepG2-NTCP cells (L).

621 **(M)** Southern blot analysis of HBV DNA in stable HBV-expressing HepAD38 cells treated as  
622 in K.

623 **(N-O)** Quantification of HBV core DNA levels in stable HBV-expressing HepAD38 cells (N)  
624 and HBV-infected HepG2-NTCP cells (O) treated as in (M) using qPCR, n=9.

625 Data are expressed as the mean  $\pm$  SD. *P* values were derived from one-way ANOVA in G-H,  
626 I-J, and N-O; (\*\*\*)*P* < 0.001).

627

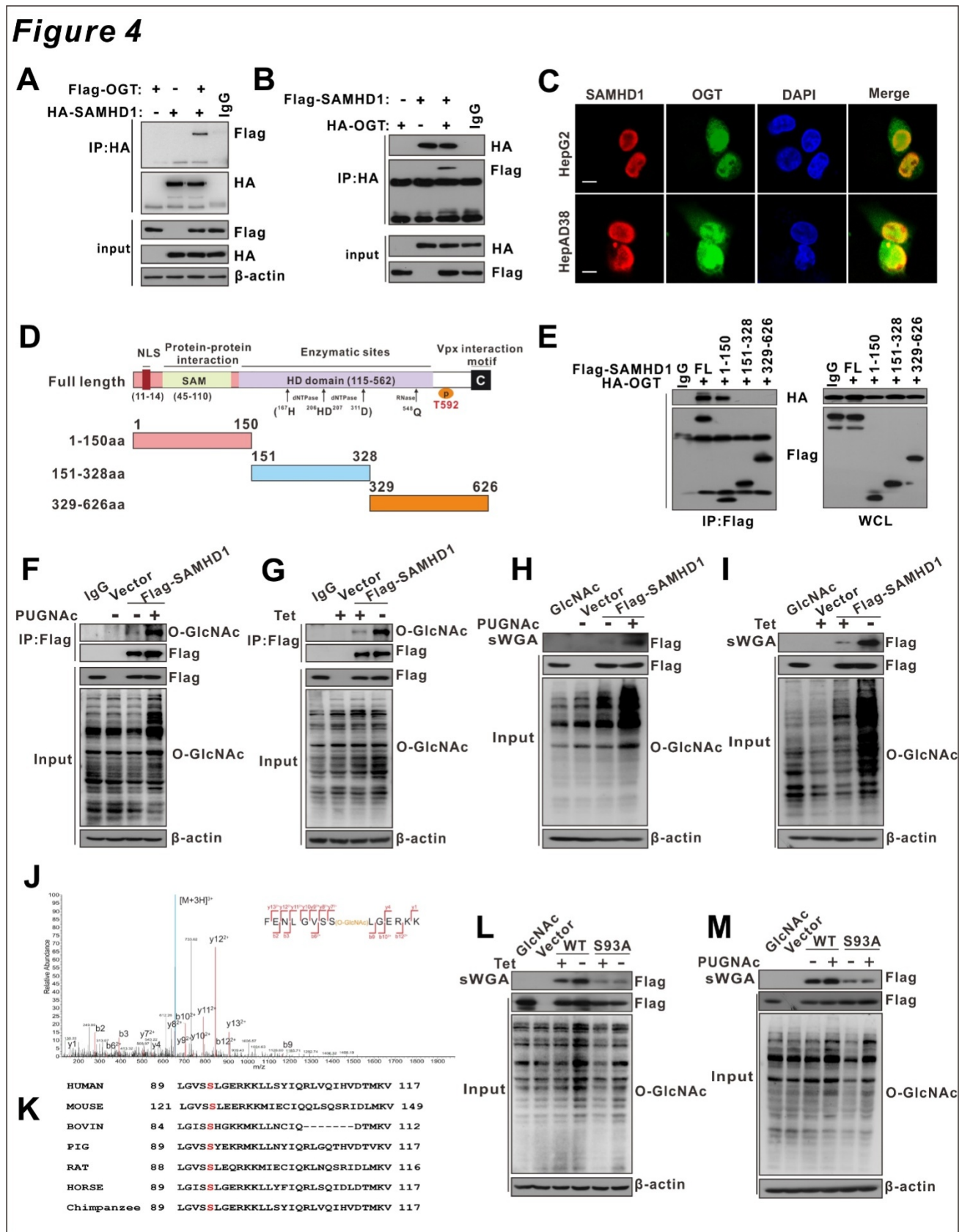


**Fig. 4. OGT mediates O-GlcNAcylation of SAMHD1 on Ser93.**

628  
629

630 (A) Immunoprecipitation (IP) of SAMHD1 with anti-HA antibody in HEK293T cells

631 co-transfected with Flag-OGT and HA-SAMHD1 expression constructs. The  
632 immunoprecipitated and input proteins were probed with the indicated antibodies.

633 **(B)** Immunoprecipitation of OGT with anti-HA antibody in HEK293T cells co-transfected with  
634 HA-OGT and Flag-SAMHD1 expression constructs.

635 **(C)** Representative confocal images of HepG2 (top) and HepAD38 cells (bottom)  
636 co-transfected with FLAG-SAMHD1 and HA-OGT. DAPI (blue) was used to counterstain  
637 nuclei. Scale bar, 10  $\mu$ m.

638 **(D-E)** The interaction between OGT and the full-length or the truncated SAMHD1 (1-150aa,  
639 151-328aa, 329-626aa), as indicated in the diagram (D), were determined by Co-IP in  
640 HEK293T cells (E).

641 **(F)** HEK293T cells were transfected with the Flag-SAMHD1 construct and the control vector  
642 for 48 h and treated with 100  $\mu$ M PUGNAc for 12 h. Following cell lysis, SAMHD1 was  
643 immunoprecipitated using anti-FLAG M2 Agarose Beads. The immunoprecipitated and input  
644 proteins were probed with an anti-O-GlcNAc or anti-Flag antibody.

645 **(G)** Immunoprecipitation of SAMHD1 with anti-Flag M2 agarose in tetracycline-inducible  
646 HepAD38 cells transfected with Flag-SAMHD1 and the control vector.

647 **(H-J)** HEK293T cells (H) were treated as in (F) and tetracycline-inducible HepAD38 cells (I)  
648 were treated as in (G). After cell lysis, O-GlcNAc-modified proteins were purified using  
649 succinylated wheat germ agglutinin (sWGA)-conjugated agarose beads and probed with an  
650 anti-Flag or anti-O-GlcNAc antibody. GlcNAc served as a negative control.

651 **(J)** LC-MS/MS analysis of FLAG-tagged SAMHD1 identified Ser93 as the SAMHD1  
652 O-GlcNAcylation site. Tandem MS spectrum of the +2 ion at m/z 508.97 corresponding to  
653 O-GlcNAcylated SAMHD1 peptide FENLGVSSLGERKK is shown.

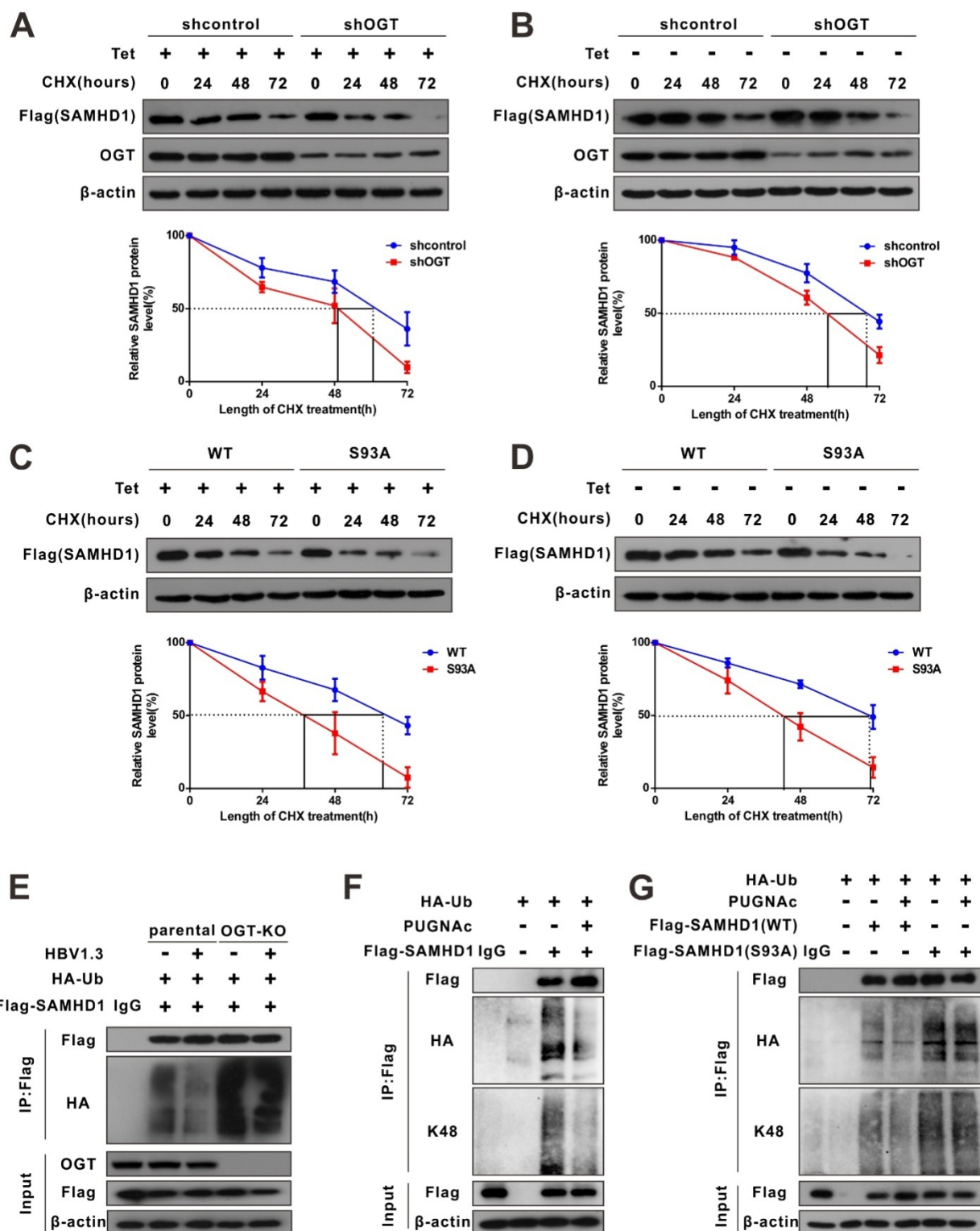
654 **(K)** Multiple sequence alignment of SAMHD1 in different species.

655 **(L-M)** SAMHD1-KO HepAD38 cells were transfected with empty vector, Flag-tagged

656 SAMHD1 WT, or S93A mutant (I). HEK293T cells were transfected with the above plasmids  
657 described in (L) and treated with 100  $\mu$ M PUGNAc for 12 h (M). Cell lysates were purified  
658 using sWGA-conjugated agarose beads and probed with an anti-Flag or anti-O-GlcNAc  
659 antibody.  
660



## Figure 5



661  
662

**Fig. 5. OGT-mediated O-GlcNAcylation on Ser93 enhances SAMHD1 stability.**

663 (A-B) Representative images of Flag-tagged SAMHD1 protein in non-infected or HBV

664 infected SAMHD1 KO HepAD38 cells. Cells were transfected with Flag-tagged SAMHD1  
665 and treated with 100  $\mu$ M CHX for the indicated time. SAMHD1 band intensity was quantified  
666 using ImageJ, n=3. CHX, Cycloheximide. KO, knockout.

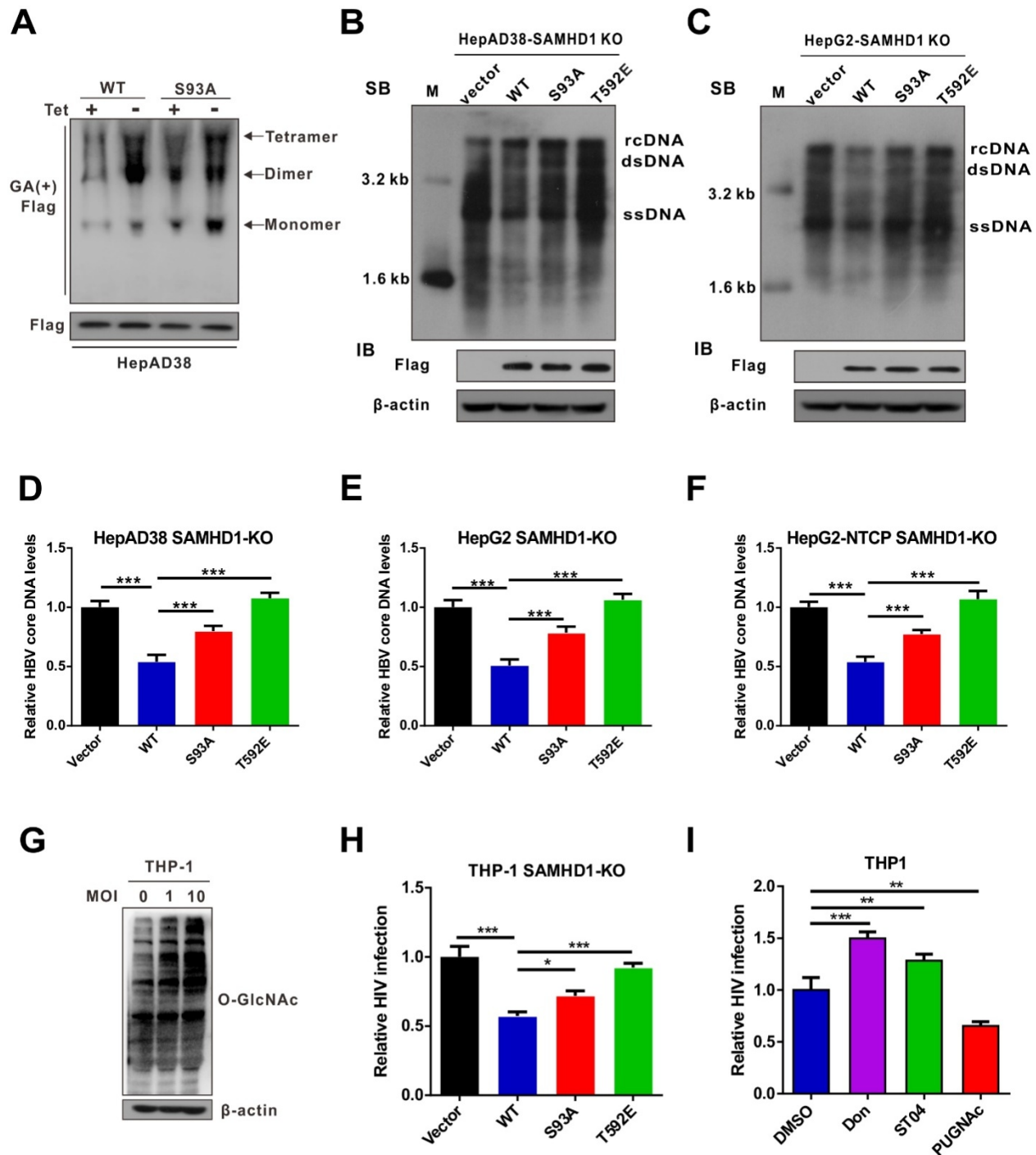
667 **(C-D)** Immunoblots of SAMHD1. SAMHD1-KO HepAD38 cells treated with (Off) or without  
668 (On) tetracycline were transfected with Flag-tagged SAMHD1 WT or S93A mutant and  
669 treated with 100  $\mu$ M CHX, n=3.

670 **(E)** SAMHD1 ubiquitination in OGT-knockout HBV-infected HepG2 cells in the presence of  
671 HA-tagged ubiquitin. After cell lysis, SAMHD1 was immunoprecipitated using anti-FLAG M2  
672 antibody. Immunoprecipitated and input proteins were probed with the indicated antibodies.

673 **(F-G)** HEK293T cells were co-transfected with HA-Ub and Flag-SAMHD1 (F), Flag-tagged  
674 SAMHD1 WT or S93A mutant (G) and treated with 100  $\mu$ M PUGNAc for 12 h. After cell lysis,  
675 SAMHD1 was immunoprecipitated using anti-FLAG M2 antibody. Immunoprecipitated and  
676 input proteins were probed with the indicated antibodies.

677

## Figure 6



678

679 **Fig. 6. O-GlcNAcylation of SAMHD1 on Ser93 is important for its antiviral activity**

680 (A) Changes in the oligomeric state of SAMHD1 upon HBV infection. SAMHD1-KO

681 HepAD38 cells with tetracycline inducible (Tet-off) HBV expression were transfected with the  
682 Flag-tagged SAMHD1 WT or S93A mutant construct. Cells were treated with glutaraldehyde  
683 (GA) and whole-cell lysates were probed with an anti-Flag antibody.

684 **(B-C)** HepAD38 cells with stable HBV-expressing (B) and HBV-infected SAMHD1-KO  
685 HepG2 cells (C) were transfected with Flag-tagged SAMHD1 WT, S93A mutant, or T592E  
686 mutant. HBV DNA levels were determined by southern blot analysis.

687 **(D-F)** SAMHD1-KO HepAD38 cells with stable HBV-expressing (D), HBV-infected  
688 SAMHD1-KO HepG2 (E) and SAMHD1-KO HepG2-NTCP cells (F) were transfected with the  
689 above plasmids described in (B). HBV core DNA levels were determined by qPCR. n=9.

690 **(G)** SAMHD1 KO-THP-1 cells were differentiated overnight with PMA (100  $\mu$ M) before  
691 infecting with HIV-LUC-G (MOI=0, 1, or 10) for 48 h. Thereafter, the cells were lysed and  
692 total O-GlcNAc levels were determined by western blotting.  $\beta$ -actin was used as a loading  
693 control.

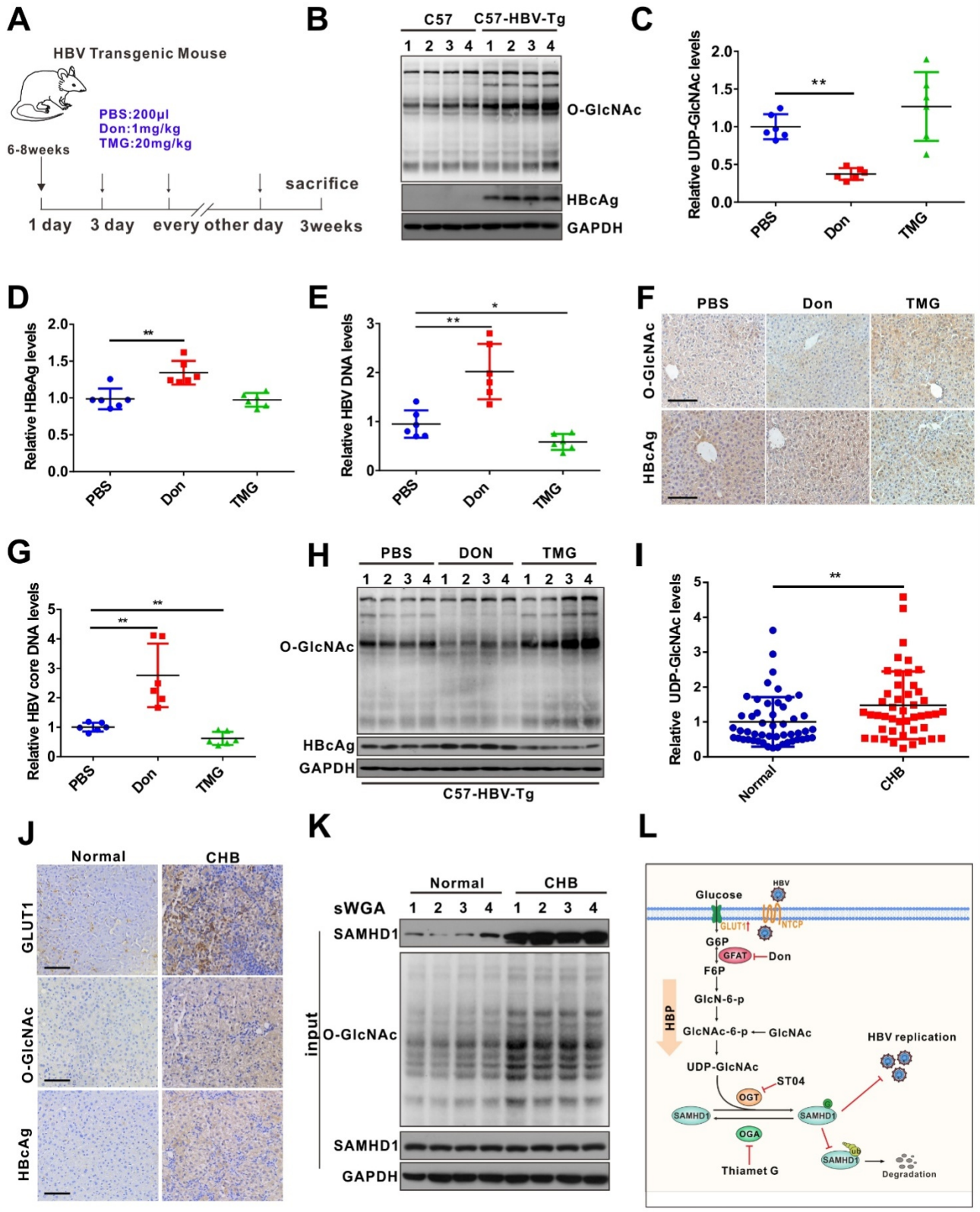
694 **(H)** SAMHD1 KO-THP-1 cells were differentiated overnight and infected with HIV-LUC-G  
695 (MOI=1) for 24 h. Thereafter, they were transfected with Flag-tagged SAMHD1 WT, S93A  
696 mutant, or T592E mutant for 48 h. Luciferase activity was measured and normalized for  
697 protein concentration. n=3.

698 **(I)** SAMHD1 KO-THP-1 cells were differentiated overnight and infected with HIV-LUC-G  
699 (MOI=1) for 24 h. Cells were then treated with Don (30  $\mu$ M, 24 h), ST04 (100  $\mu$ M, 24 h), or  
700 PUGNAc (100  $\mu$ M, 48 h), and luciferase activity was measured. n=3.

701 Data are expressed as the mean  $\pm$  SD. *P* values were derived from one-way ANOVA in D-F,  
702 H-I. (\* *P*<0.05, \*\* *P*<0.01, \*\*\**P*<0.001).

703  
704

## Figure 7



705

706

**Fig. 7. HBV infection promotes UDP-GlcNAc biosynthesis and protein**

707

**O-GlcNAcylation *in vivo***

708 (A) Six- to eight-week-old HBV transgenic mice were intraperitoneally injected with Don (1  
709 mg/kg body weight) and TMG (20 mg/kg body weight) or PBS (control) every other day for  
710 10 times. The mice were sacrificed on day 20 post-treatment.

711 (B) Immunoblotting of total O-GlcNAc in HBV transgenic mice.

712 (C) Fold change in the expression of UDP-GlcNAc in mouse liver tissues was determined by  
713 UHPLC-QTOF-MS. n=6 per group.

714 (D-E) Serum HBeAg and HBV DNA levels in mice. n=6 per group.

715 (F) O-GlcNAc and HBcAg detection in mouse liver tissues, Scale bar, 50  $\mu$ m.

716 (G) Quantification of HBV core DNA levels in mouse liver tissues using qPCR. n=6.

717 (H) Immunoblot of total O-GlcNAc in HBV transgenic mice treated as in (A).

718 (I) Fold change in the expression of UDP-GlcNAc in the liver tissues of patients with CHB  
719 was determined by UHPLC-QTOF-MS. (Normal=50, CHB=46).

720 (J) GLUT1, O-GlcNAc, and HBcAg detection in liver tissue specimens from patients with  
721 CHB. Scale bar, 50  $\mu$ m.

722 (K) Liver tissue lysates from patients with CHB were purified using sWGA-conjugated  
723 agarose beads and probed with an anti-SAMHD1 or anti-O-GlcNAc antibody.

724 (L) Proposed working model of this study.

725 Data are expressed as the mean  $\pm$  SD. *P* values were derived from one-way ANOVA in C-E,  
726 G, and from unpaired, two-tailed Student's *t*-test in I. (\* *P*<0.05, \*\* *P*< 0.01).

727  
728